

Growth of metal micro and/or nanoparticles utilizing arc-discharge immersed in liquid

B. Rebollo-Plata^a, M. P. Sampedro^{b*}, G. Gallardo-Gómez^a, N. Ortega-Miranda^a, C. F. Bravo-Barrera^c,
G. Daniel-Pérez^a, B. Zenteno-Mateo^d, D. Hernández-Cruz^e and S. Jiménez-Sandoval^f

^a*Instituto Tecnológico Superior de Irapuato,*

km 12.5 Carr. Irapuato-Silao, Irapuato Guanajuato, 36821, México.

^b*Facultad de Ingeniería Química, Benemérita Universidad Autónoma de Puebla,*
Av. San Claudio y 18 Sur Edif. 106 D, Ciudad Universitaria, Puebla, 72590, Puebla, México,
**e-mail: mpstraviata@hotmail.com*

^c*Comisión Federal de Electricidad – Laboratorio de Pruebas de Equipos y Materiales,*
Irapuato, Guanajuato, México.

^d*Facultad de Ingeniería, Benemérita Universidad Autónoma de Puebla,*
Boulevard Valsequillo y Circuito CU, Ciudad Universitaria, Puebla, Puebla, 72590, México.

^e*Facultad de Ingeniería, Universidad Autónoma de Chiapas, Chiapas, México.*

^f*Centro de Investigación y de Estudios Avanzados del IPN,*
Laboratorio de Investigación en Materiales, Querétaro, México.

Received 22 Octubre 2013; accepted 18 March 2014

In this paper, we present results on the metal microcrystals and nanoparticles of Al, Cu and Al-Cu composite growth by arc-discharge with the system immersed in distilled water, under different conditions and varying the current from 50 to 150 A with constant voltage (27 V). These structures are characterized using X-ray diffraction, scanning electron microscopy, Raman spectroscopy and Uv-Vis spectroscopy. Our results demonstrate that metal micro and nanostructures can be prepared at low cost with high quality.

Keywords: Metal microcrystals and/or nanoparticles; distilled water; arc-discharge immersed in liquid.

PACS: 81.05.Mh; 81.05.Ni; 81.05.Pj; 81.05.Qk; 78.30.Er; 81.16.Pr; 68.37.Hk

1. Introduction

The study of oxides and metal nanoparticles with different sizes has been extremely active, during the last decade, mainly due to the many interesting and different properties compared with the materials in bulk [1]. Aluminum oxide is a material with technological importance because it has a wide band gap (~ 9.9 eV), chemical stability and interesting mechanical properties. Many structural changes in the aluminum oxide have been reported, with the phase Al_2O_3 being the most stable thermodynamically at room temperature and pressure [2]. Also copper oxides have been synthesized creating copper oxides in two phases: Cu_2O and CuO , both are p-type semiconductors, they are synthesized by oxidation [3]. Nanosystems of copper aluminates have fundamental importance for different purposes due to their large superficial area. Typically, the superficial area is related to small size particles that produces high mechanical resistance, hydrophobicity and low superficial acid value [4,5]. Reported results have proved that the ultrafine particles and nanocrystals have high resistance to be worn away for different coefficients of friction [6].

Recently, different groups have synthesized high quality micro and nano metallic oxides, using different techniques, such as: DC oxygen plasma [7], plasma engineering [8], soft-chemistry approaches [9], high energy pulsed plasma arc [10], wire explosion process [11]. The most common tech-

niques for copper oxides synthesis are: chemical vapor nucleation [12], intense pulsed light [13], arc-discharge [14]; and for aluminum-copper particles are: ultrasonic sonochemistry [15], CVD [16], spin-on [17], DC sputtering [18]. Among other applications these structures have been used in tunnel junction devices [19-22], barrier pinholes [23], acute toxicological effects [24], to reduce friction and wear [25], glucose sensor [26], transparent electronic [27], and other applications.

The aim of this work is to grow micro and nanoparticles of aluminum oxide (Al), copper oxide (Cu) and aluminum/copper composite (Al/Cu) using the arc-discharge immersed in a distilled water system. This technique has not been used for the synthesis of these types of micro and nanostructures, besides we demonstrate the possibility to obtain particles with high quality and at low cost.

2. Experimental Procedure

Arc-discharge systems use electrodes which are commercial cylindrical bars or rods of aluminum and copper with 7.5 cm length and 1 to 6 mm in diameter, respectively. The electrodes are cleaned with acetone, prior to be used; then they are placed in front of each other at a distance of 1 mm. The smaller electrode is fixed while the other can be displaced back and forth. The system creates plasma at different current values: 50, 75, 100 and 150 A; at constant voltage (27 V). To

preserve the plasma a knob is used, in order to displace manually the “mobile” bar, and therefore conserve the distance between both bars. The technique uses a rectangular container made up of pyrex, where the electrodes are submerged to a depth of 6 cm, in distilled water. The experiment lasts at least 5 minutes. During the experiment, the nanoparticles can be found in three zones: a) at the bottom of the container, due to the precipitation (zone 1), b) floating on the surface (zone 2) and c) floating around the intermediate zone of the container (zone 3).

After collecting the metallic and bimetallic nanoparticles, from each of the three zones by means of a pipette they are placed in three smaller containers. Then, each of these three containers is exposed to a sonication process for 60 minutes. The sonication helps to better disperse and select the particles. Thereafter, some drops from each container are placed on a silicon substrate and then are taken for morphological and structural analysis.

3. Results and Discussion

In order to investigate the properties and characteristics of the particles, from the three zones, different techniques have been used. A scanning electron microscope (Quanta 200 3D, FEI) has been used to explore the morphology, combined with EDS, for elemental chemical analysis. An X-Ray Diffractometer (Bruker) has been used to determine the crystallinity of the material and, a Raman Spectrometer (Lab Raman II Dillor) for the structural properties. Finally, a UV-Vis spectrophotometer (Cary 50 Conc, Varian) has been used to determine the optical absorption of the particles. Once these analyses are performed, one is able to select the best particles, from the best zone.

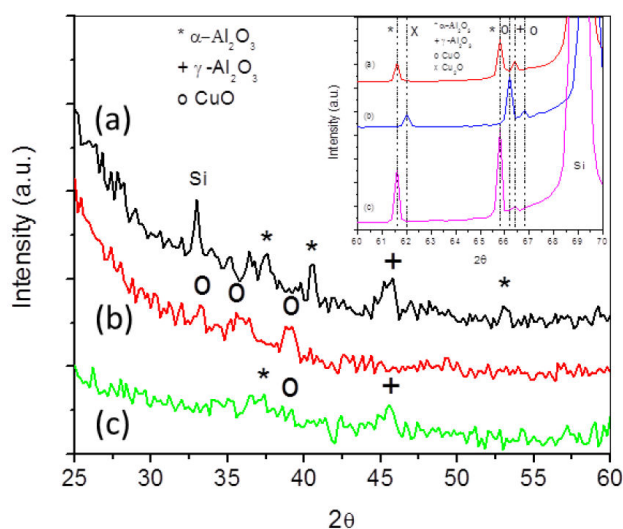


FIGURE 1. Typical pattern of X-ray diffraction of nanoparticles: a) aluminum oxide, b) copper oxide and c) composite Al-Cu/O, prepared by arc-discharge using 150 A (zone 2), in these diffractograms are shown different phases of these materials.

3.1. X Rays Diffraction

3.1.1. Aluminum particles

Figure 1 shows the representative pattern of X-rays of aluminum nanoparticles, grown by an arc-discharge at 150 A. The different peaks present in the diffractogram are attributed basically to two phases: α - Al_2O_3 peaks (denoted with *) are for the big crystalline grains; and the other peaks are for the phase γ - Al_2O_3 with the peaks denoted with (+), formed by the dehydration and the progressive desorption of hydroxyl groups from the nanoparticles surface. These phases can be observed in the inset for 2θ measurements for the range between 60-70 degrees. Our results are similar to those reported in [28-31].

3.1.2. Copper particles

Particles of copper have been grown under similar conditions to those of aluminum particles. In the diffractogram (Fig. 1) the particles exhibit crystalline peaks, with basically two phases present: CuO denoted with (o) and Cu_2O with (x), these results are similar to those reported in [32-36].

3.1.3. Bimetallic particles of aluminum/copper

Although it was difficult to identify the phases in the Al-Cu/O composite, due to the tendency to the amorphous state, according to the low intensity values in the 2θ measurements, however we have been able to detect the crystalline phase, between 60 and 70 degrees (see inset in Fig. 1).

These results demonstrate that the arc-discharge system is a good alternative technique for the growth of metal and bimetallic oxide particles of different sizes in crystalline and amorphous phase at low cost and high quality.

3.2. Scanning Electron Microscopy (SEM)

3.2.1. Microcrystals and nanoparticles of oxide copper

During the sample preparation, one can observe particles in three zones of the experiment: a) Precipitated at the bottom of the container, b) suspended particles in the solution, and c) on the surface of the liquid. Samples from those three areas were taken and examined with the SEM. The micrographs shown in Fig. 2 depict the morphology of the copper oxide particles which precipitate at the bottom of the container (zone 1). Here we can observe the spherical structures these particles have, characteristic of the grown particles by the arc-discharge technique [14]. The diameters are in the range of 50-150 μm and most of them have “defects” on the surface or they are “punctured” or both (Fig. 2a). On the surface of those spheres there are micrometric (~ 1 -2 μm) crystals and nanometric (~ 40 -900 nm) particles of oxide copper with different architectures (Fig. 2b). The elemental chemical analysis, performed by EDS, indicates a composition of 15.90% of oxygen and 84.10% of copper, this result confirms

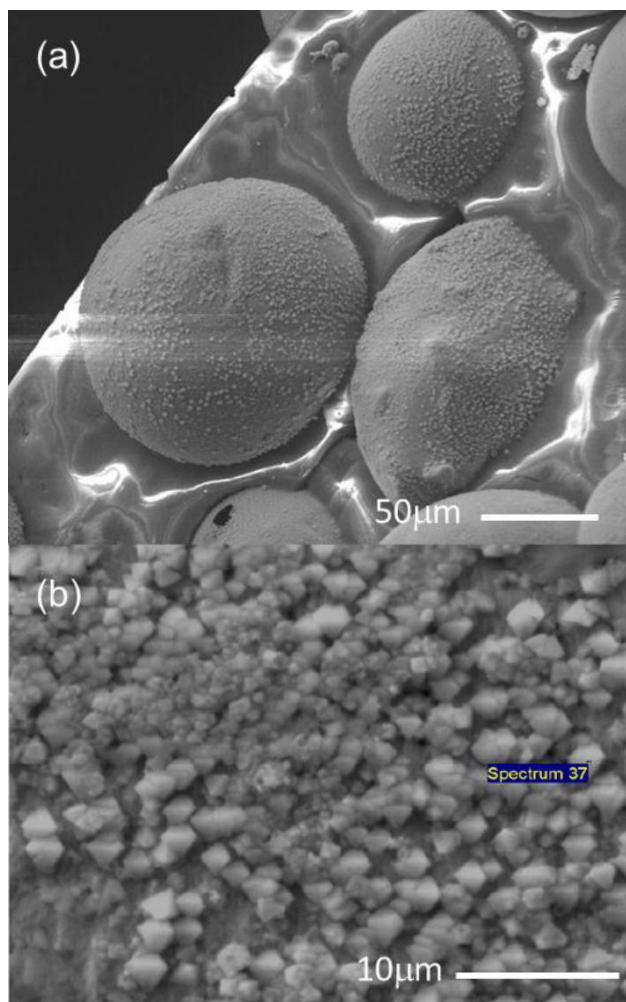


FIGURE 2. a) Micrograph of oxide copper spheres whose diameter is in the range of 50-150 μm , with microcrystals on the surface and b) amplification of micro and microcrystals oxide copper on the surface. These spheres and crystals are precipitated in the bottom of container (zone 1).

that the crystals and nanoparticles oxides of copper are favored by the environment, rich in oxygen. Dispersing the suspended particles (zone 2 was chosen before zone 3 by the amount of particles obtained) by sonication, one can observe clearly nanoparticles of copper oxide (see Fig. 3a), the elemental chemical analysis, made by EDS, indicates a composition of 49.85% of oxygen and 50.15% of copper. These results have been obtained in experiments where we have varied the current in a range within 50-150 A. The figures were obtained from particles grown at 150 A. Preparation of these microcrystals using the arc-discharge technique, to our knowledge, has not been studied before.

3.2.2. Nanoparticles of oxide aluminum

Results obtained of the aluminum oxide are different from those of copper oxide particles, these are in part due to the fact that spheres have smaller diameters nevertheless spheres were embedded in the surface where there are only particles

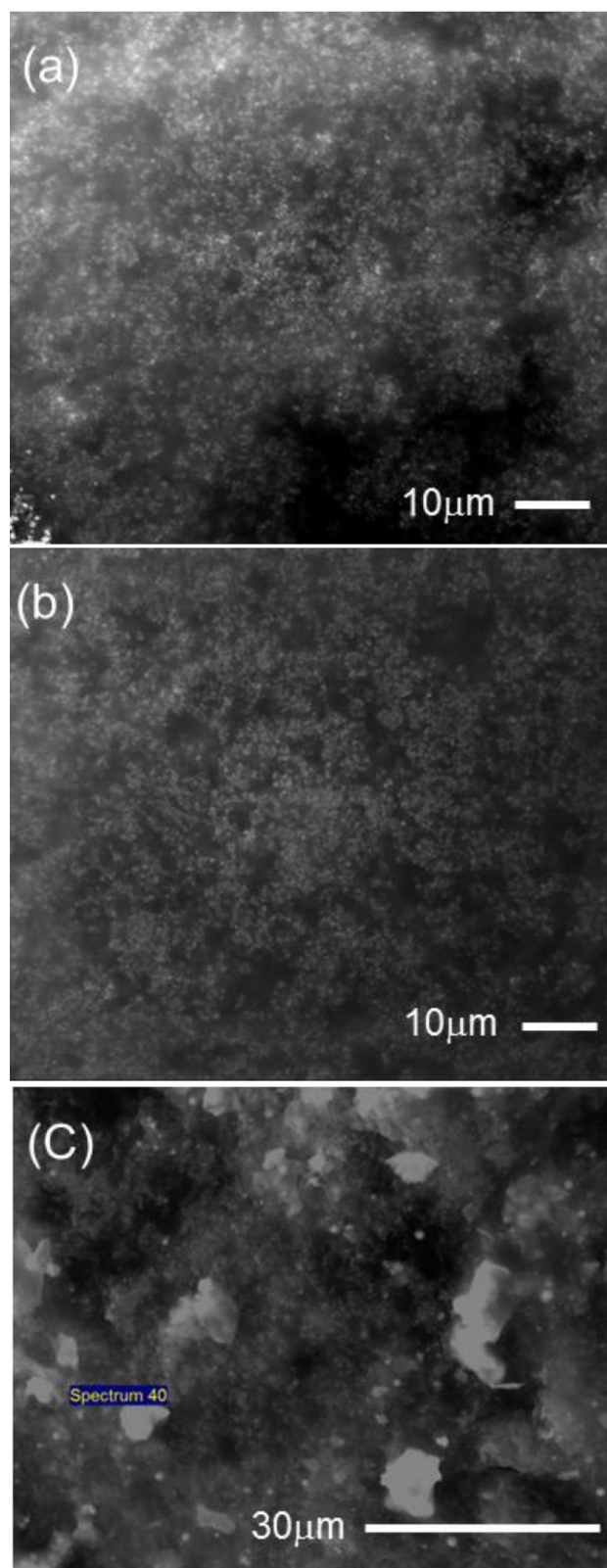


FIGURE 3. Micrographs of metal nanoparticles grown by arc-discharge: a) aluminum oxide with basic chemical analysis using EDX (O:96%, Al:4%), b) for copper oxide, chemical analysis (O:91.4%, Cu:8.6%) and c) aluminum-copper bimetallic nanoparticles, chemical analysis (O:49.22%, Al:40.28%, Cu:10.50%). These nanoparticles are suspended in the solution (zone 2).

of aluminum oxide but no nanocrystals (zone 1). Using this technique to explore copper metallic particles (see Fig. 3b) we have detected particles with similar size whose composition is 66.14% of oxygen and 33.86% of aluminum.

3.2.3. Bimetallic Particles of Aluminum and Copper

We have also prepared bimetallic aluminum/copper particles with this technique (see Fig. 3a), results show the cluster formation. Using chemical analysis (EDS) we have determined that these particles contain 49.22% of oxygen, 40.28% of aluminum and 10.50% of copper. This analysis has been also performed for particles in zone 2.

4. Raman spectroscopy

4.1. Aluminum oxide particles

Figure 4 shows Raman spectra of the oxide nanoparticles: a) aluminum, b) copper and c) aluminum/copper. The aluminum oxide particles (see Fig. 4a) show two principal peaks at 111 and 222 cm^{-1} which correspond to AlO; and at 461 and 737 cm^{-1} for $\alpha\text{-Al}_2\text{O}_3$, these results are consistent with those reported in [8, 28], where the shift and width of the Raman peaks are attributed to grain size. Peaks located at ~ 300 , 500 and 950 cm^{-1} , correspond to the substrate, as reported in [39, 40].

4.2. Copper oxide particles

In the Raman spectra of copper oxide particles depicted in Fig. 4b there are peaks at 75 and 121 cm^{-1} which correspond to CuO and another peak at 275 cm^{-1} for Cu_2O , these results are similar to those reported in [41-43].

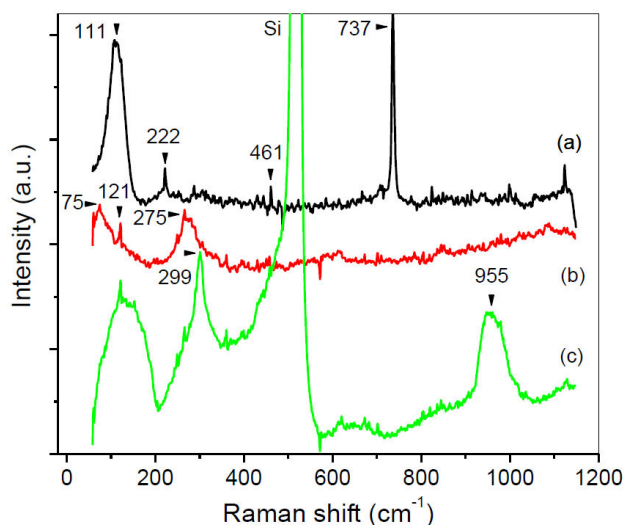


FIGURE 4. Raman spectra of oxide nanoparticles: a) aluminum, b) copper and c) composite aluminum/copper, created utilizing the arc-discharge method immersed in distilled water (zone 2), in these spectra different phases can be seen of the material, this strengthens the previous results.

4.3. Aluminum/copper oxide particles

In the Raman spectra of the bimetallic oxide particles shown in figure 4c, we observe a broad band centered at $\sim 135 \text{ cm}^{-1}$ ($58\text{-}208 \text{ cm}^{-1}$), which can be related to AlO and CuO composites. Note the presence of the peak at 121 cm^{-1} which is attributed to CuO as mentioned above; also there is another peak at 299 cm^{-1} , which was not present in the copper spectra and attributed to CuO. In this spectrum, there is an additional peak located at 955 cm^{-1} , this peak is attributed to Si-OH related to the substrate, as mentioned above.

The above discussion shows that the signatures of these metal and bimetallic particles are mainly located below 1000 cm^{-1} , as mentioned in various previous reports.

4.4. Uv-Vis spectroscopy

The optical transmittance/absorbance spectra ($\sim 300\text{-}800 \text{ nm}$) of the oxide particles: a) aluminum, b) copper and c) aluminum/copper prepared by the arc-discharge system are represented in Fig. 5. This figure shows representative transmittances for particles grown at 150 A, we find transmittance between 30 and 50 for Al particles, between 50 and 75 for Cu particles and between 30 and 80 for Al/Cu particles. From these results it is seen that bimetallic particles have a higher transmittance and aluminum particles have the lowest.

The optical band gap values obtained from the absorption coefficient for aluminum particles varies from 2.67 to 3.45 eV, for copper particles varies from 3.39 to 3.94 eV and for bimetallic particles varies from 2.82 to 3.95 eV. The possible origin of the optical band gap increase is the decrease in particle size, as mentioned in [44-45].

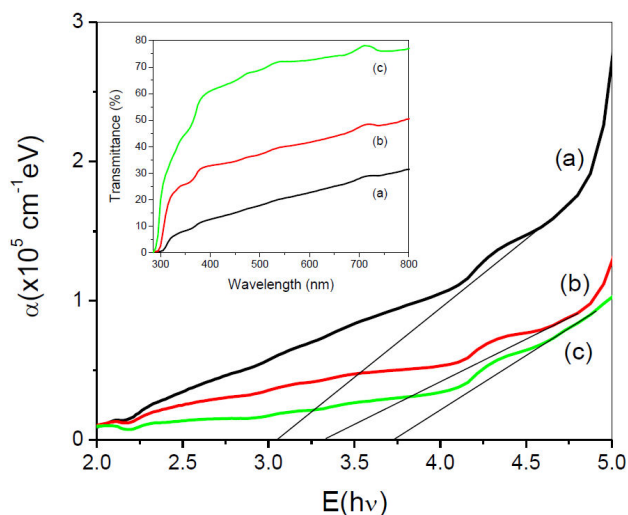


FIGURE 5. Uv-Vis transmittance spectra of oxide nanoparticles: a) aluminum, b) copper and c) aluminum/copper composite, prepared using the arc-discharge immersed in distilled water (zone 2). These spectra show that the transmittance for bimetallic nanoparticles is the largest and that also results in a greater band gap.

5. Conclusions

It has been demonstrated that the electric discharge technique immersed in distilled water is a potential technique for the growth of different metallic and bimetallic materials, with different sizes as processes are controlled. In this paper, microcrystals and nanoparticles of different metals such as aluminum, copper and Al/Cu composites (Al/Cu) have been grown, at low cost with high quality. To our knowledge there

are no previous reports of some results presented in this paper, which increases the relevance of our findings.

Acknowledgments

The authors are grateful to T. S.A. Roa-Medina, M.E. J. Díaz-Méndez, S. Padilla-Vargas and M.C. E.Q. Saavedra-Arroyo for technical assistance and to M.S.I. M.R. Arzate-Mosqueda for the institutional assistance.

1. D.L. Feldheim, and C.A. Foss Jr., *Metal Nanoparticles: Synthesis, Characterization, and Applications*, (Marcel Dekker, New York, 2002).
2. O. Ozuna, G.A. Hirata, and J. McKittrick, *J. Phys.: Condens. Matter*. **16** (2004) 2585-2591.
3. A. Chen, H. Long, X. Li, Y. Li, G. Yang, and P. Lu, *Vacuum* **XXX 1-4** (2008).
4. M. Kevin, W.L. Ong, G.H. Lee, and G.W. Ho, *Nanotechnology* **22** (2011) 235701.
5. W. Lv, Z. Luo, H. Yang, B. Liu, W. Weng, and J. Liu, *Ultrasonics Sonochemistry* **17** (2010) 344–351.
6. Y.S. Zhang, K. Wang, Z. Han, K. Lu, *J. Mater. Res.* **23** (2008) 150.
7. J.A. Baier-Saip, J.I. Avila, G. Tarrach, A.L. Cabrera, V. Fuenzalida, R.A. Zarate, I.K. Schuller, *Surf. Coat. Tech.* **195** (2005) 168-175.
8. T. Laha, K. Balani, A. Agarwal, S. Patil, and S. Seal, *Metallurgical and Materials Transactions A* **36** (2005) 301.
9. H.Y. Zhu, X.P. Gao, D.Y. Song, and S.P. Ringer Y.X. Xi.
10. K. Kim., *Metals and Materials International* **14** (2008) 707-711.
11. T.K. Sindhu, R. Sarathi, and S.R. Chakravarthy, *Bull., Mater. Sci.* **30** (2007) 187-195.
12. A.G. Nasibulin, P.P. Ahonen, O. Richard, E.I. Kauppinen, and I.S. Altman, *Nanoparticle Research* **3** (2001) 385–400.
13. J. Ryu, H.S.G. Kim, and H.T. Hahn., *J. Electronic Materials* **40** (2011) 42.
14. S.Y. Xie, Z.J. Ma, C.F. Wang, S.C. Lin, Z.Y. Jiang, R.B. Huang, and L.S. Zheng, *J. Solid State Chemistry* **177** (2004) 3743–3747.
15. W. Lv, Z. Luo, H. Yang, B. Liu, W. Weng, and J. Liu, *Ultrasonics Sonochemistry* **17** (2010) 344-351.
16. H. Gong, Y. Wang, and Y. Luo, *Appl. Phys. Lett.* **76** (2001) 3959.
17. S. Gao, Y. Zhao, P. Gou, N. Che, and Y. Xie, *Nanotechnology* **14** (2003) 538.
18. A.N. Banerjee, and K.K. Chattopadhyay, *J. Appl. Phys.* **97** (2005) 084308.
19. J.M. Daughton, *Thin Solid Films* **216** (1992) 162.
20. D.E. Heim, R.E. Fontana Jr., C. Tsang, V.S. Speriosu, B.A. Gurney, and M.L. Williams, *IEEE Trans. Magn.* **30** (1994) 162.
21. B.J. Jonsson-Akerman, R. escudero, C. Leighton, S. Lim, I.K. Schuller, and D.A. Rabson, *Appl. Phys. Lett.* **77** (2000) 1870.
22. B.F.P. P.A. Beck, S.O. Democritov, and B. Hillebrands, *Surf. Sci.* **497** (2002) L55.
23. J.J. Akerman, I.K. Schuller, J.M. Slaughter, and R.W. Dave, *Appl. Phys. Lett.* **79** (2001) 1.
24. Z. Chen *et al.*, *Toxicology Letters* **163** (2006) 109-120.
25. G. Liu, X. Li, B. Qin, D. Xing, Y. Guo, and R. Fan, *Tribology Lett.* **17** (2004) 961-966.
26. Q. Xu, Y. Zhao, J.Z. Xu, and J.J. Zhu, *Sensors and Actuators B* **114** (2006) 379-386.
27. A. Banerjee, and S.W. Joo, *Nanotechnology* **22** (2011) 1-8.
28. S. Cava, S.M. Tebcherani, I.A. Souza, S.A. Pianaro, C.A. Paskocimas, E. Longo, and J.A. Varela, *Materials Chemistry and Physics* **103** (2007) 394–399.
29. Q. Fu, C.B. Cao, and H.S. Zhu, *Thin Solid Films* **348** (1999) 99-102.
30. O. Ozuna, G.A. Hirata, and J. McKittrick, *J. Phys.: Condens. Matter*. **16** (2004) 2585-2591.
31. T. Laha, K. Balani, A. Agarwal, S. Patil, and S. Seal, **36A** (2005) 301.
32. M. Yin, C.K. Wu, Y. Lou, C. Burda, J.T. Koberstein, Y. Zhu, and S. O'Brien. *J. Am. Chem. Soc.* **127** (2005) 9506-9511.
33. A. Chen, H. Long, X. Li, Y. Li, G. Yang, and P. Lu, *Vacuum*, **xxx** (2008) 1-4.
34. M. Kevin, W.L. Ong, G.H. Lee, and G.W. Ho, *Nanotechnology*, **22** (2011) 235701.
35. A.G. Nasibulin, P.P. Ahonen, O. Richard, E.I. Kauppinen, and I.S. Altman, *Journal of Nanoparticle Research* **3** (2001) 385-400.
36. S.Y. Xie, Z.J. Ma, C.F. Wang, S.C. Lin, Z.Y. Jiang, R.B. Huang, and L.S. Zheng, *Journal of Solid State Chemistry* **177** (2004) 3743-3747.
37. T. Laha, K. Balani, A. Agarwal, S. Patil, and S. Seal, *Metallurgical and Materials Transactions A* **36A** (2005) 301.
38. S. Cava *et al.*, *Materials Chemistry and Physics* **103** (2007) 394–399.
39. P.A. Temple and C.E. Hathaway, *Phys. Rev. B* **7** (1973) 3685-3697.

40. X. Gao and I.E. Wachs, *Journal of Catalysis* **192** (2000) 18-28.
41. T. Wei, Master Degree Thesis, (Simon Fraser University, 1990).
42. J. Trajic *et al.*, *Acta Physica Polonica A* **117** (2010) 791.
43. M.A. Khan, T.P. Hogan, and B. Shanker, *J. Nano Systems & Technology* **1** (2009) 1.
44. J. Pellicer-Porres, A. Segura, A.S. Gilliland, A. Muñoz, P. Rodríguez-Hernández, D. Kim, M.S. Lee and T.Y. Kim, *Appl. Phys. Lett.* **88** (2006) 181904.
45. K. Li, J.F. Huang, L.Y. Cao, B. Wang, and Z.Y. Shi, *Journal of Inorganic Materials* **26** (2011).